Coherent acoustic phonon generation in exciton self-trapping

F. X. Morrissey and S. L. Dexheimer*
Department of Physics and Astronomy, Washington State University, Pullman, Washington 99164, USA
(Received 1 January 2010; published 22 March 2010)

The coupled electronic and vibrational dynamics of exciton self-trapping are studied in the quasi-one-dimensional material $[Pt(en)_2][Pt(en)_2Br_2]\cdot(PF_6)_4$ (en=ethylenediamine) using femtosecond impulsive excitation techniques. We report transient absorption measurements at 77 K that are modulated by a large amplitude, strongly damped oscillatory component at a frequency of 11 cm^{-1} in addition to the 110 cm^{-1} excited-state optical-phonon wave-packet oscillation previously observed at room temperature. We find that the characteristics of the low-frequency oscillatory response are consistent with the theoretically predicted generation of a propagating coherent acoustic wave accompanying the formation of the localized lattice deformation that stabilizes the self-trapped state. The observed low-frequency oscillation, interpreted in the context of theoretical models for polaron formation via coupling to acoustic phonons, provides an estimate of the spatial extent of the resulting localized state of ~5 unit cells of the PtBr chain structure. This value is in good agreement with the localization length predicted by previous extended Peierls-Hubbard calculations.

DOI: 10.1103/PhysRevB.81.094302 PACS number(s): 71.35.Aa, 78.47.−p, 78.67.−n

I. INTRODUCTION

The localization of an electronic excitation via interaction with a deformable lattice is a process of fundamental interest in a wide range of condensed-matter systems, and has a dramatic impact on the optical and transport properties of materials. An important example is the formation of a self-trapped exciton (STE, also referred to as an exciton-polaron): an initially excited extended free-exciton state interacts with the lattice, resulting in the formation of a localized STE state, in which the exciton is stabilized in a localized lattice deformation; this process is directly analogous to the formation of a lattice polaron from an initially delocalized electron.[1] In the case of an ideal one-dimensional lattice, the transition from the extended free state to the localized self-trapped state is theoretically predicted to be a barrierless process so that the dynamics of the photoinduced structural rearrangement associated with exciton self-trapping are extremely rapid, occurring on the time scale of a single vibrational period. In this work, we use femtosecond vibrationally impulsive excitation, in which the system is excited with an optical pulse short compared to the periods of the relevant vibrational modes, to time resolve the coupled electronic and lattice dynamics inherent to the self-trapping process. We present transient absorption measurements at low temperature that reveal a large amplitude, strongly damped, low-frequency oscillatory modulation that accompanies STE formation. We find that the characteristics of the low-frequency oscillatory response provide evidence for the generation of a coherent acoustic wave as the lattice deforms during the localization process. This is a physical phenomenon that has been predicted and modeled theoretically, but to our knowledge, this process has not previously been experimentally identified. Moreover, comparison of the observed response to previous theoretical modeling of the dynamics of polaron formation via coupling to acoustic phonons in one dimension[2] provides a means to estimate the spatial extent of the resulting localized state, a key property for the physics of the localization process, and one that has not generally been accessible in previous experimental work.

The measurements reported here are carried out on the $[Pt(en)_2][Pt(en)_2Br_2]\cdot(PF_6)_4$ [also referred to as PtBr(en), en=ethylenediamine, $C_2H_8N_2$] mixed-valence metal-halide (*MX*) linear-chain complex. The *MX* complexes are a class of quasi-one-dimensional materials that have proven to be excellent model systems for investigating the physics of electron-phonon coupled systems.[3] The basic structural motif is a covalently bonded, extended linear chain of alternating transition-metal ions (*M*) and halide ions (*X*) that defines the quasi-one-dimensional geometry. The transition-metal ions are also coordinated by transverse ethylenediamine ligands, and PF_6^- counterions spatially separate parallel metal-halide chains in the crystal structure so that the crystalline materials retain a quasi-one-dimensional character. The ground electronic state is a Peierls-distorted charge-density wave with alternating valence states on the metal ions and corresponding alternation in the metal-halide bond lengths, and the structure along the chain axis can be represented schematically as $\ldots$—X^--$M^{+(3+\delta)}$-X^-—$M^{+(3-\delta)}$—X^--$M^{+(3+\delta)}$-X^-—$M^{+(3-\delta)}$—$\ldots$. The complexes have a strong optical intervalence charge-transfer (IVCT) transition that effectively transfers charge between inequivalent metal sites. The final state of this electronic transition, the free exciton, is delocalized along the chain axis and rapidly evolves into a localized STE through its interaction with the lattice. The resulting STE state consists of a localized region in which the charge-density wave is absent or reduced and the Peierls distortion of the metal-halide bond lengths is accordingly relaxed. In general, the spatial extent of the STE in the *MX* complexes is expected to depend on the relative strengths of the electron-phonon and electron-electron interactions, which vary across the *MX* series. The actual spatial extent of the STE in the PtBr(en) complex has not previously been definitively determined but numerical calculations based on extended Peierls-Hubbard models have predicted that the structural distortion should extend over a number of unit cells.[3]

Femtosecond impulsive excitation techniques, which probe the dynamics of vibrations coupled to an optical exci-

tation, have been applied to studies of exciton self-trapping in *MX* materials in a number of previous studies.[4–12] In these measurements, the material is excited using optical pulses short compared to the periods of its characteristic vibrations, creating vibrational wave packets that consist of a coherent superposition of vibrational states, and the evolution of the vibrational wave packets is detected as an oscillatory modulation of the optical response.[13] In impulsive excitation pump-probe measurements on *MX* complexes, the formation of the STE following excitation of the IVCT transition is detected by monitoring the appearance of its characteristic redshifted absorbance, and the associated vibrational dynamics are detected as an excited-state wave-packet oscillation that accompanies the formation of the STE absorbance. In our previous trasinet absorption experiments on PtBr(en),[4,5] carried out at room temperature, we detected an excited-state wave-packet oscillation at a frequency of 110 cm^{-1} that damps as the STE absorbance forms on a time scale of ~300 fs. Detailed measurements at detection wavelengths throughout the STE absorption band provided a picture of the excited-state dynamics in which the 110 cm^{-1} oscillation corresponds to a lattice motion that carries the excited system from the initial ground-state structure to the distorted structure of the self-trapped state. Given the strong coupling of the Raman-active symmetric stretch ground-state optical-phonon mode to the IVCT transition, the photoinduced lattice dynamics are expected to include a strong component of this relative motion of the metal and halide ions, though the observed excited-state oscillation frequency is shifted relative to the 177 cm^{-1} ground-state Raman frequency. Additional recent transient absorption and time-resolved luminescence measurements on *MX* materials[6–12] have also shown similar wave-packet motion; however, a detailed understanding of the localization mechanism remained to be realized, including, in particular, the nature and spatial extent of the lattice deformations that stabilize the localized state.

Although clear excited-state processes are observed in the room-temperature experiments described above, thermally induced effects may be expected to contribute both to the degree of initial lattice disorder and to thermally induced vibrational dephasing processes, potentially obscuring additional components of the dynamics. Recent impulsive excitation studies[7,10] on PtBr(en) at cryogenic temperatures have revealed additional low-frequency oscillations; however, the nature of these oscillations, including their relation to the physics of the localization process, was not established. In the work reported here, we present systematic studies of the low-frequency vibrational dynamics and comparison with simple physical models to allow an interpretation of the low-frequency response as acoustic wave generation inherent to the self-trapping process.

II. EXPERIMENT

Wavelength-resolved impulsive excitation pump-probe measurements were carried out as described previously.[5] Briefly, the complex was excited at the low-energy side of the IVCT transition using pulses 35 fs in duration centered at 800 nm from a 1 kHz Ti:sapphire regenerative amplifier, and the resulting change in transmission was probed using a compressed white-light continuum. Wavelength resolution was achieved by spectrally filtering the probe beam following transmission through the sample. A portion of the continuum was split off for use as a separately detected reference to correct for intensity fluctuations of the probe pulses. Use of the reference for noise reduction, together with signal averaging, allowed acquisition of signals with noise levels $\sim 0.0005 \Delta T/T$.

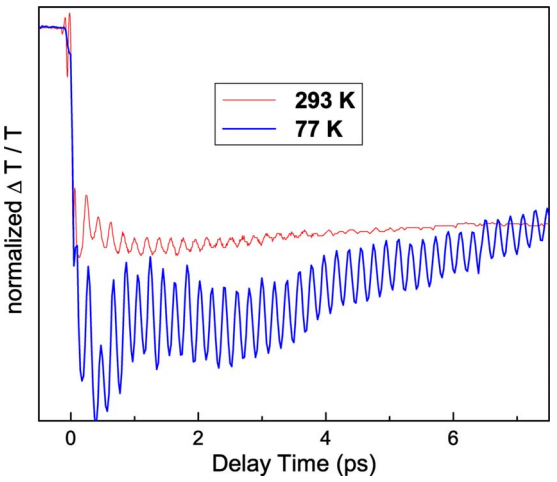

FIG. 1. (Color online) Comparison of the time-resolved differential transmittance of $[Pt(en)_2][Pt(en)_2Br_2]\cdot(PF_6)_4$ at 293 and 77 K following excitation of the optical intervalence charge-transfer transition with pulses 35 fs in duration centered at 800 nm, probed within the self-trapped exciton absorption band at a detection wavelength of 940 nm using a compressed continuum. Signals are normalized to their values at 7.5 ps.

The experimental samples were single crystals of $[Pt(en)_2][Pt(en)_2Br_2]\cdot(PF_6)_4$ of good optical quality. Measurements on $[Pt(en)_2][Pt(en)_2Br_2]\cdot(ClO_4)_4$, which differs only in the counterion that separates the parallel PtBr(en) chains in the crystal, were also made for comparison. The materials were prepared using recent advances in the synthesis of the metal-halide complexes that produce crystals that are largely free of defects and that are resistant to photoinduced damage.[14,15] For both counterions, single crystals form in the shape of elongated trapezoidal plates, with the chain axis lying in the plane of the plate parallel to the long edge. Crystals were mounted on 1-mm-thick sapphire plates in a cold finger cryostat.

III. RESULTS

A comparison of the time-resolved optical response of a single-crystal sample of $[Pt(en)_2][Pt(en)_2Br_2]\cdot(PF_6)_4$ following impulsive excitation of the IVCT transition at room temperature (293 K) and at 77 K is presented in Fig. 1. The measurements in Fig. 1 were carried out at a detection wavelength of 940 nm, within the redshifted absorption band of the STE. Both the pump and probe pulses were polarized along the chain axis. The resulting signals appear as a negative differential transmittance, corresponding to an induced absorbance following excitation.

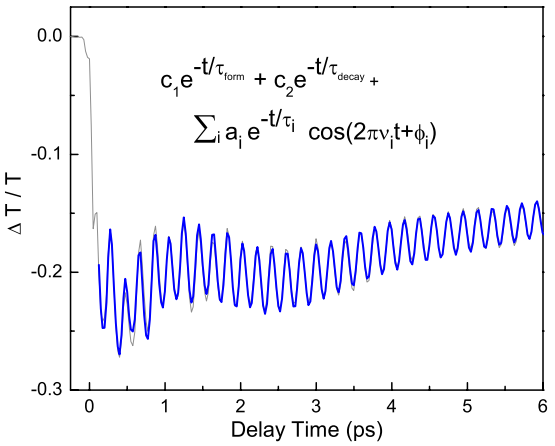

FIG. 2. (Color online) Measured differential transmittance at 77 K data (narrow gray line) with a fit (heavy line) to a sum of exponentially damped oscillations and exponential formation and decay components, as described in the text. Signals near zero time delay include nonlinear contributions from pump-probe pulse overlap and are not included in the analysis.

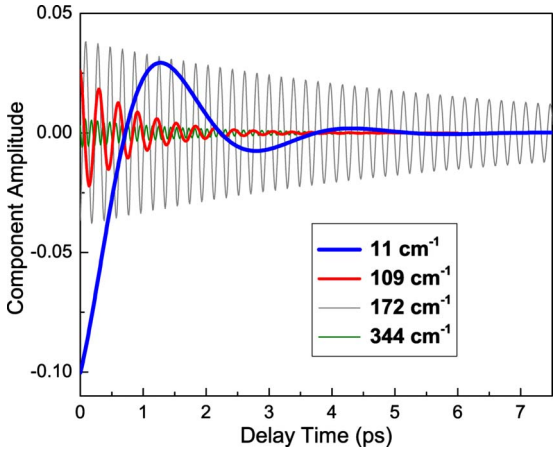

FIG. 3. (Color online) Individual oscillatory components constructed from the fit parameters in Table I.

The room-temperature response consists of the components reported previously.[4] An exponential formation component reflects the formation of the STE induced absorbance on a time scale of ~300 fs, and is followed by a slow decay reflecting loss of the metastable STE population. The induced absorbance is modulated by a rapidly damped excited-state vibrational wave-packet oscillation at a frequency of 110 cm^{-1}. In addition, the pump-probe response includes ground-state wave-packet oscillations generated by the resonantly enhanced stimulated impulsive Raman mechanism that appear at the ground-state Raman frequency of 177 cm^{-1} and its second harmonic at 354 cm^{-1}. The response measured at 77 K includes these components with the addition of a large amplitude, strongly damped, low-frequency modulation. In Fig. 2, the low-temperature measurement is characterized by fitting the response to the sum of exponential formation and decay functions together with a sum of exponentially damped oscillations,

$$\Delta T(t)/T = c_1 \exp(-t/\tau_{form}) + c_2 \exp(-t/\tau_{decay}) + \sum_i a_i \exp(-t/\tau_i)\cos(2\pi\nu_i + \phi_i). \quad (1)$$

The individual oscillatory components determined by the fit are presented in Fig. 3, and the fit parameters are reported in Table I. We note that while other functional forms may be considered for the dynamics, we find that these simple exponential functions provide an excellent characterization of the time-resolved response. Four oscillatory components were included to account for the previously established ground-state Raman frequency and its second harmonic and the established excited-state frequency at 110 cm^{-1}, together with a new component for the low-frequency oscillation that appears at low temperature. Starting parameters for the multiparameter nonlinear fits were determined by linear prediction singular-value decomposition analysis[16] and by Fourier transformation. These three methods for determination of the frequency components gave generally consistent results; we report the nonlinear fitting results in Table I since this method also provides uncertainty limits.

From the fit results for the measurements at 77 K, we find that the low-frequency modulation in the low-temperature response appears at a frequency of 11 cm^{-1}, within the range characteristic of acoustic phonons. The remaining signal components are consistent with previous modeling of room-temperature response.[4] The exponential formation component again reflects the finite formation time of the STE induced absorbance, which then slowly decays as the metastable STE population returns to the ground state. Wave-packet modulation is again observed at the excited-state frequency of ~110 cm^{-1}, and interestingly, we find an increased dephasing time at 77 K (840 fs as compared with the rapid ~300 fs room-temperature dephasing time). The oscillatory modulation at 172 cm^{-1} and its second harmonic at 344 cm^{-1} are again consistent with excitation of ground-state vibrational wave packets by the resonantly enhanced stimulated impulsive Raman mechanism, in which both the observed increase in dephasing time and the small downward shift in frequency of the ground-state oscillations at low temperature are consistent with the expected temperature dependence of the ground-state Raman response.[17]

The response at 77 K was measured at a series of detection wavelengths within the absorption band of the STE, and no significant variation in the low-frequency oscillatory component of the response was observed. To investigate the possibility that the photoinduced dynamics may include compo-

TABLE I. Fit parameters for oscillatory components of Eq. (1). Error values are in parentheses. For the formation and decay components, τ_{form}=250 (30) fs, τ_{decay}=12.6 (0.2) ps, c_1=−0.288 (0.005), and c_2=−0.247 (0.001).

Frequency ν (cm^{-1})	Damping time τ (fs)	Amplitude a	Phase ϕ (deg)
11 (0.3)	1100 (100)	0.10 (0.01)	182 (7)
109 (1)	840 (100)	0.026 (0.002)	1 (6)
171.5 (0.1)	6100 (300)	0.0393 (0.0008)	180 (2)
344 (1)	1600 (500)	0.006 (0.002)	−14 (10)

nents transverse to the chain axis, measurements were also carried out with probe pulses polarized perpendicular to the chain axis; no signal was observed in this case. No significant differences were observed in PtBr(en) crystallized with the two different counterions PF_6^- and ClO_4^-, as expected for a response involving dynamics along the Pt-Br chain axis.

IV. DISCUSSION

The physics of self-trapping of electronic excitations via interaction with a deformable lattice has been treated theoretically in a number of limiting cases, reflecting the type and strength of the electron-phonon interaction.[1] In principle, both optical and acoustic phonons can be involved in the electron-phonon interactions that drive the self-trapping process. In this and previous studies of PtBr(en), the observed modulation at 110 cm^{-1} has been assigned to optical-phonon dynamics associated with self-trapping corresponding to relative motions of the metal and halide ions.[4,5,9] In general, for self-trapping via acoustic interactions, acoustic phonons with a range of q vectors may couple to the electronic excitation to create the lattice deformation that stabilizes the self-trapped state, with dominant contributions expected from phonon modes of wavelength $\lambda = 2\pi/q$ on the order of the spatial extent of the exciton. The dispersion of the phonon branch allows energy dissipation in the lattice, and in particular, in the case of self-trapping via coupling to acoustic phonons, the energy associated with stabilization of the exciton is released as propagating acoustic waves.[18,19]

The evolution of the lattice deformation during the process of polaron formation in an acoustic chain has been modeled by Brown *et al.*,[2,20] who carried out calculations of the dynamics of a system consisting of an electronic excitation with a linear electron-phonon coupling to a one-dimensional lattice with an acoustic dispersion relation using many-body techniques. Their results are shown schematically in Fig. 4, which presents graphs of the lattice displacements along the one-dimensional chain at a series of time delays as the system evolves following photoexcitation. The lattice dynamics reflect the radiation of energy as the polaron forms, where in this simple model, the energy is seen to be radiated as two counterpropagating acoustic pulses that are replicas of the deformation that forms around the polaron. Although their model involves the simplifying assumptions of coupling to a single phonon branch and the limit of negligible electronic transport, it captures the essential physics of the generation of propagating coherent acoustic waves as an integral part of the dynamics of self-trapping involving coupling to acoustic modes.

We find that the characteristics of the observed 11 cm^{-1} modulation are in good agreement with this mechanism of generation of coherent acoustic waves during self-trapping. The acoustic dynamics presented in Fig. 4 imply a means to find the spatial extent, or localization length, of the self-trapped state: since the acoustic waves are replicas of the lattice deformation, and since the spatial extent of the electronic wave function is expected to follow that of the lattice deformation (for example, as seen in the calculations of Gammel *et al.*, Ref. 3), the acoustic frequency should yield a

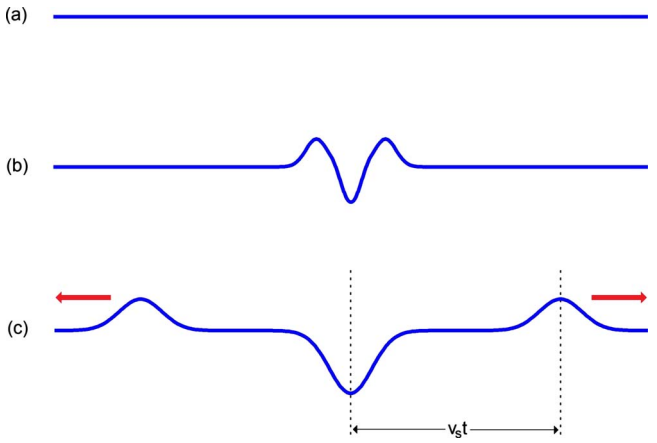

FIG. 4. (Color online) Schematic representation of the acoustic phonon generation process associated with self-trapping of an electronic excitation coupled to an acoustic phonon mode in a one-dimensional lattice. Traces represent the displacement of the lattice from equilibrium as a function of distance along the one-dimensional lattice at a series of time delays following photoexcitation. (a) Undisturbed lattice at $t=0$. (b) Formation of the lattice deformation. (c) Counterpropagating acoustic pulses in the form of replicas of the lattice deformation that stabilizes the self-trapped electronic excitation. After Brown *et al.*, Ref. 2.

measure of the localization length. Comparison of the observed oscillatory response with this model requires a numerical value for the acoustic velocity along the chain axis. This was determined by numerical calculation of the longitudinal-phonon dispersion relations for a linear lattice with an effective four-atom unit cell representing the Peierls-distorted —Br-Pt-Br—Pt— chain-axis repeat unit, with the slope of the acoustic branch at the zone center yielding the acoustic velocity. The dispersion relations were calculated by simultaneous solution of the coupled equations of motion for longitudinal motions of this four-atom unit including both nearest-neighbor and next-nearest-neighbor interactions, using force constants determined by Love *et al.*[21] from modeling of Raman and far-infrared vibrational spectroscopic measurements. The resulting value of the acoustic velocity along the chain axis $v_s = 5.7$ km/s so that the observed 11 cm^{-1} oscillation frequency corresponds to an acoustic wavelength of 17 nm. Since the acoustic wave predicted in Ref. 2 appears as an approximately half-cycle pulse, we take the full width at half maximum (FWHM) of a half cycle of the acoustic wavelength as a measure of the spatial extent of the deformation of the lattice. The resulting estimated localization length $\ell_{\mathrm{FWHM}} = 5.7$ nm corresponds to five —Br-Pt-Br—Pt— chain-axis repeat units of the PtBr(en) structure.[17] This value is in remarkably close agreement with the theoretical prediction of Gammel *et al.*,[3] who carried out numerical calculations of the properties of nonlinear excitations in PtBr and related materials using extended Peierls-Hubbard techniques with Hamiltonian parameters estimated from spectroscopic and structural data. Though these calculations are necessarily approximate, given the simplification of the Hamiltonian and estimation of some Hamiltonian parameters, the match to a localization length that extends over a significant number of unit cells is notable.

The observed dephasing time of the low-frequency oscillation is also consistent with this mechanism of generation of coherent acoustic waves during the self-trapping process. If the observed low-frequency oscillation is considered as a modulation of the STE induced absorbance by the coherent acoustic pulse, the transit time of the acoustic wave through the spatial extent of the exciton would be expected to be a dominant contribution to the lifetime of the observed oscillation. The sound velocity and FWHM values determined above give a simple estimate of the transit time of $\ell_{\mathrm{FWHM}}/v_s = 1.0$ ps. This result is in good agreement with the observed damping time of 1.1 ps for the 11 cm^{-1} oscillation, providing a self-consistent picture for the low-frequency dynamics.

We note that the observed 11 cm^{-1} oscillation is not consistent with generation of coherent acoustic phonons by the well-established mechanism of laser-induced heating. In this process, which was first identified in metal and semiconductor films,[22] local heating resulting from optical generation of hot electronic excitations by the pump pulse followed by equilibration with the lattice can create a local thermal stress. This in turn can generate an acoustic pulse that propagates away from the excited surface of the sample, with the width and effective wavelength of the acoustic pulse on the order of twice the optical-absorption length ζ of the pump excitation. The heating-induced stress mechanism for coherent acoustic phonon generation requires that the heating resulting from the pump excitation take place on a time scale much shorter than the period of the acoustic wave so as to impulsively excite the acoustic motion; typical time scales for dissipation of electronic energy into heat are too slow to meet this condition for our observed oscillation period of 3 ps. Moreover, in the present experiment, the optical-absorption depth is too long and the observed oscillation period is too short to be consistent with the heating-induced strain mechanism. Since the pump wavelength of 800 nm lies near the onset of the intervalence charge-transfer band in PtBr(en), the absorption depth is relatively long. Optical constants for PtBr(en) at the pump wavelength measured at 77 K yield an absorption depth of[23] 200 nm so that this mechanism would give rise to an acoustic wave of wavelength $2\zeta \approx 400$ nm, corresponding to a much lower frequency than is observed. In the heating mechanism for generation of coherent acoustic waves, coupling of the probe pulse to the propagating strain wave launched from the sample surface can result in a detected oscillation period of[22] $T_{\mathrm{heating}} = \lambda_{\mathrm{probe}}/2nv_{\mathrm{sn}}$, where v_{sn} is the sound velocity in the direction normal to the sample surface. To our knowledge, the acoustic velocity in this crystal direction has not been determined for PtBr(en); however, v_{sn} may be estimated from the chain-axis v_s value above using the ratio of the acoustic velocities parallel and perpendicular to the chain axis determined for the related *MX* material PtI(en) in the inelastic neutron-scattering studies of Bardeau *et al.*[24] This gives an estimated oscillation period for a heating mechanism in PtBr(en) of $T_{\mathrm{heating}} \sim 100$ ps, much longer than the observed period of 3 ps. Finally, the observation of a similar response in both $[\mathrm{Pt(en)_2}][\mathrm{Pt(en)_2Br_2}]\cdot(\mathrm{PF_6})_4$ and $[\mathrm{Pt(en)_2}][\mathrm{Pt(en)_2Br_2}]\cdot(\mathrm{ClO_4})_4$ crystals is also inconsistent with the heating-induced strain mechanism. These crystals differ only in the counterion, which is located between parallel PtBr chains in the crystal structure. $\mathrm{ClO_4^-}$ gives stronger hydrogen-bonding interactions than $\mathrm{PF_6^-}$ and also has a different mass so that different frequencies would be expected for waves propagating transverse to the chain in these two crystals.

Following our initial report of a low-frequency oscillatory modulation of the femtosecond transient absorption response in PtBr(en),[7] Yasukawa *et al.*[10] reported a low-frequency component detected in $[\mathrm{Pt(en)_2}][\mathrm{Pt(en)_2Br_2}]\cdot(\mathrm{ClO_4})_4$ via time-resolved photoluminescence, which they model in terms of a configuration coordinate system with two degrees of freedom. They propose the possibility that the low-frequency component could correspond to motion along a coordinate leading to formation of soliton pairs. This assignment is speculative, given that it is not clear whether the potential-energy surface is bound along such a coordinate, which would be necessary for an oscillation to occur, nor whether the energetics of the soliton states in PtBr(en) are conducive to such a decay mechanism. We note that we have recently detected a large amplitude, strongly damped, low-frequency oscillation in low-temperature transient absorption measurements on the *MX* linear-chain complex $[\mathrm{Pt(en)_2I_2}][\mathrm{Pt(CN)_4}]$ that is remarkably similar to that seen in PtBr(en), aside from a small change in frequency that is consistent with a different acoustic velocity and STE localization length in the iodide-bridged material.[25] In this material, the chain consists of Pt ions with alternating ethylenediame and CN transverse ligands that pin the charge-density wave so that the ground state is nondegenerate, and therefore, soliton excitations do not exist. The good agreement between the characteristics of the low-frequency oscillation with the coherent acoustic wave mechanism discussed above, as well as the observation of a low-frequency response that is strikingly similar to that in PtBr(en) in a material that does not support soliton excitations, argue against a soliton-based mechanism as the origin of the low-frequency oscillation.

The low-frequency component in the luminescence response is reported as a frequency of 0.7 THz (23 cm^{-1}) based on Fourier transformation and 0.6 THz (20 cm^{-1}) based on fitting results. Both of these values are higher than the 11 cm^{-1} oscillation frequency found in the transient absorption measurements reported here. The origin of this difference is difficult to definitively ascertain, though we note two differences between the two studies that may affect the determination of the frequency of this strongly damped component: the analysis of the transient absorption measurements presented here includes a finite formation time for the STE induced absorbance consistent with that established in previous time-resolved studies of exciton dynamics in PtBr(en);[4,5] in addition, the transient absorption measurements do not show evidence of the discontinuity apparent in the luminescence traces at a delay time near 2.5 ps; instead, a broad minimum is found that corresponds to the second minimum of the low-frequency oscillation. We also expect that the determination of the signal components may be aided by the high signal-to-noise ratio achieved in the transient absorption measurements, together with the excellent fit to the simple oscillatory response function of Eq. (1).

While simple physical models for self-trapping mechanisms generally involve only a single type of electron-

phonon interaction,[1] the results presented here indicate that both acoustic and optical phonons are involved in exciton self-trapping in the *MX* materials. In addition to providing an observation of the acoustic mode dynamics, which were likely obscured by thermally induced lattice disorder and dephasing processes in room-temperature studies, the low-temperature measurements provide further insight into the dynamics involving the 110 cm^{-1} excited-state optical-phonon mode. The analysis of the 77 K response shown in Fig. 2 reveals a nearly threefold increase in the dephasing time for the 110 cm^{-1} excited-state vibrational coherence as compared to the previously observed room-temperature dephasing time of ~300 fs, indicating that the rapid vibrational dephasing dynamics of the optical mode at room temperature are in part, thermally induced, rather than being entirely intrinsic to the excited-state structural change. Together, the two observed oscillatory components associated with the self-trapping dynamics indicate that the structural transition to the STE state involves both motion of the bridging halide ions away from the asymmetric positions characteristic of the Peierls-distorted ground state (corresponding to the mode with optical-phonon character at 110 cm^{-1}) along with a longer wavelength lattice deformation over a spatial extent of ~5 unit cells, corresponding to the acoustic mode at 11 cm^{-1}.

V. CONCLUSION

In conclusion, we have probed the coupled electronic and vibrational dynamics associated with exciton self-trapping in a quasi-one-dimensional system at low temperature, and report a dramatic observation of low-frequency lattice dynamics accompanying STE formation. We find that the low-frequency response is consistent with the generation of coherent acoustic phonons as an integral part of the localization dynamics. We demonstrate that the low-frequency response is inconsistent with the previously established mechanism of laser-induced heating for the generation of coherent acoustic waves; the mechanism discussed here represents a distinct mechanism for the generation of coherent phonons in the condensed phase. These results, interpreted in the context of theoretical models for polaron formation in one-dimensional systems, provide further insight into the nature of the self-trapped state and its formation dynamics. In particular, the acoustic frequency provides a measure of the spatial extent of the resulting localized state, a key property for understanding the localization physics.

ACKNOWLEDGMENTS

We gratefully acknowledge J. A. Brozik and W. E. Buschmann for preparing single-crystal PtBr(en) samples. We thank S. Mukamel for bringing Ref. 2 to our attention, and M. D. McCluskey for assistance with calculation of phonon-dispersion relations. This work is supported by the NSF under Grants No. DMR-0305403 and No. 0706407.

*Corresponding author.

[1] Reviewed in, E. I. Rashba in *Excitons*, edited by E. I. Rashba and M. D. Sturge (North-Holland, New York, 1982), p. 543.
[2] D. W. Brown, K. Lindenberg, and B. J. West, J. Chem. Phys. **84**, 1574 (1986).
[3] J. T. Gammel, A. Saxena, I. Batistic, A. R. Bishop, and S. R. Phillpot, Phys. Rev. B **45**, 6408 (1992). The STE corresponds to the neutral biexciton in this work.
[4] S. L. Dexheimer, A. D. Van Pelt, J. A. Brozik, and B. I. Swanson, Phys. Rev. Lett. **84**, 4425 (2000).
[5] S. L. Dexheimer, A. D. Van Pelt, J. A. Brozik, and B. I. Swanson, J. Phys. Chem. A **104**, 4308 (2000).
[6] A. D. Van Pelt and S. L. Dexheimer, *Ultrafast Phenomena XII*, Springer Series in Chemical Physics Vol. 66, edited by T. Elsaesser, S. Mukamel, M. Murnane, and N. F. Scherer (Springer-Verlag, Berlin, 2001), p. 393.
[7] F. X. Morrissey and S. L. Dexheimer, OSA Trends Opt. Photonics Ser. **89**, QThJ18 (2003).
[8] S. Tomimoto, S. Saito, T. Suemoto, K. Sakata, J. Takeda, and S. Kurita, Phys. Rev. B **60**, 7961 (1999).
[9] S. Tomimoto, S. Saito, T. Suemoto, J. Takeda, and S. Kurita, Phys. Rev. B **66**, 155112 (2002).
[10] K. Yasukawa, Y. Takahashi, S. Kurita, and T. Suemoto, Solid State Commun. **140**, 197 (2006).
[11] A. Sugita, T. Saito, H. Kano, M. Yamashita, and T. Kobayashi, Phys. Rev. Lett. **86**, 2158 (2001).
[12] Y. Wada, N. Matsushita, and H. Haneda, J. Lumin. **108**, 285 (2004).
[13] L. Dhar, J. A. Rogers, and K. A. Nelson, Chem. Rev. (Washington, D.C.) **94**, 157 (1994).
[14] J. A. Brozik, B. L. Scott, and B. I. Swanson, Inorg. Chim. Acta **294**, 275 (1999).
[15] W. E. Buschmann, S. D. McGrane, and A. P. Shreve, J. Phys. Chem. A **107**, 8198 (2003).
[16] F. W. Wise, M. J. Rosker, G. L. Millhauser, and C. L. Tang, IEEE J. Quantum Electron. **23**, 1116 (1987).
[17] S. C. Huckett, B. Scott, S. P. Love, R. J. Donohoe, C. J. Burns, E. Garcia, T. Frankcom, and B. I. Swanson, Inorg. Chem. **32**, 2137 (1993).
[18] Y. Toyozawa, Prog. Theor. Phys. **26**, 29 (1961).
[19] Y. Toyozawa, in *Relaxation of Elementary Excitations*, edited by R. Kubo and E. Hanamura (Springer-Verlag, New York, 1980), p. 3.
[20] D. W. Brown, K. Lindenberg, and B. J. West, J. Chem. Phys. **87**, 6700 (1987).
[21] S. P. Love, S. C. Huckett, L. A. Worl, T. M. Frankcom, S. A. Ekberg, and B. I. Swanson, Phys. Rev. B **47**, 11107 (1993).
[22] C. Thomsen, H. T. Grahn, H. J. Maris, and J. Tauc, Phys. Rev. B **34**, 4129 (1986).
[23] Y. Wada and M. Yamashita, Phys. Rev. B **42**, 7398 (1990).
[24] J.-F. Bardeau, A. Bulou, B. I. Swanson, and B. Hennion, Phys. Rev. B **58**, 2614 (1998).
[25] J. Mance and S. L. Dexheimer (unpublished).